Photostability Study of Inverted Polymer Solar Cells Under AM 1.5G and LED Illumination via Impedance Spectroscopy

ALFONSINA ABAT AMELENAN TORIMTUBUN[ID] [1], **JOSÉ G. SANCHEZ**[ID] [2],
JOSEP PALLARÈS[ID] [1] **(Senior Member, IEEE), AND LLUIS F. MARSAL**[ID] [1] **(Senior Member, IEEE)**

1 Department of Electrical Electronic Engineering and Automatic, Universitat Rovira i Virgili, 43007 Tarragona, Spain
2 Institute of Chemical Research of Catalonia, Barcelona Institute of Science and Technology (ICIQ-BIST), 43007 Tarragona, Spain

CORRESPONDING AUTHOR: L. F. MARSAL (e-mail: lluis.marsal@urv.cat)

ABSTRACT The use of polymer solar cells (PSCs) for indoor dim-light energy harvesting has attracted significant interest for low power consumption electronics such as the Internet of Things. However, the photostability study and degradation mechanism under indoor artificial light is far behind than those under full sun illumination (standard AM 1.5G), which is crucial for the successful commercialization of indoor PSCs. Herein, the operational lifetime and photodegradation mechanism of PTB7-Th:PC$_{70}$BM-based inverted PSCs degraded under standard AM 1.5G and 1000 lux LED 2700K light sources were compared. A high power conversion efficiency (PCE) of up to 16.19% and a long operational lifetime (T$_{80}$) of 3060 min were achieved by LED-irradiated devices, higher and more stable than that of AM 1.5G-irradiated devices with PCE of 9.98% and T$_{80}$ of only 260 min. Using impedance spectroscopy and three resistive-capacitive equivalent circuit model, we were able to identify the most suffered layer. Our results demonstrate that PSCs have potential practical applications as high performance and a high stable indoor power source.

INDEX TERMS Polymer solar cells, photostability, AM 1.5G, LED light, impedance spectroscopy.

I. INTRODUCTION

The development of polymer solar cells (PSCs) as indoor dim-light energy harvesting has recently attracted great interest in powering low-power wireless connected Internet of Things (IoT) [1]–[3]. It is forecasted that about 28 billion smart devices, such as sensors, small displays, and actuators, will be connected into the IoT networks by 2021 [4]. As these low-power consumption electronic devices are usually operated indoors, PSCs can be ideal alternative to provide local power supply by harvesting light from an indoor environment. The unique features of cost-effective, lightweight, flexible, environmentally benign, and coloration of PSCs are highly desirable for indoor applications [5]–[7]. Due to their highly tunable light-absorption photoactive materials properties and well-matched spectral response between the absorption spectra of PSCs device with the

emission spectra of common indoor light sources, such as fluorescence and light-emitting diode (LED) lamps, PSCs have shown as much higher power conversion efficiency (PCE) under dim-light illumination [8]–[10]. A recent study by Nam *et al.* demonstrated that PSCs cells illuminated under 1000 lux LED light could possess max PCE of 26.4%, almost three times higher than those under one sun illumination (9.34%) [11].

Besides high PCE, stability is another vital factor for achieving commercial application of PSCs technology [12]–[15]. Extrinsic degradation in the presence of water and oxygen, intrinsic degradation in the dark, and intrinsic photo-induced degradation are dynamic aging mechanisms that may affect the stability of PSCs [16]–[18]. The development of encapsulation technologies makes it now possible to control the extrinsic degradation [19]. However,

the cells are still degraded intrinsically over time, even with perfect encapsulation. In PSCs, semiconductor polymers are generally degraded under sunlight irradiation in the absence of oxygen and moisture [20], [21]. Hence, studying the intrinsic photostability of PSCs under an inert atmosphere is particularly interesting, as it provides a more solid understanding of the process involved in the absence of a substance that could chemically alter the photoactive materials [22]. Doumon *et al.* showed that the solar irradiation-induced degradation of polymer:fullerene solar cells in the inert condition is mainly due to the ultraviolet (UV) components of the solar spectrum affecting the operational lifetime of polymers with different chemical structure [21]. A recent study by Gasparini *et al.* also suggested that the full sun illumination light-induced trap formation may cause open-circuit voltage (V_{OC}) losses [23]. In addition, severe burn-in phenomenon has been widely observed at the beginning of the photodegradation under sunlight and inert environment in PSCs, which lead the PCE drops exponentially [24]–[26]. Although the photostability of PSCs under 1 sun illumination has been reported in several studies, the photodegradation mechanism of PSCs under LED light as a common artificial indoor light source has rarely been studied, which is worth noting that the application of indoor PSCs in IoT is surging. Therefore, a rigorous understanding of the photostability of PSCs under LED illumination is urgently needed.

Different optoelectronic techniques are used to monitor degradation and gain insights into degradation mechanisms within the device [27], [28]. Impedance spectroscopy (IS) in particular can measure the complex dielectric properties of the material by perturbing a small frequency-modulated (AC) signal on the direct current (DC) bias voltage in terms of frequency spectrum [29]. The extracted frequency-dependent impedance can be interpreted in terms of the equivalent circuits model with resistive/capacitive (RC) elements to describe the internal process of PSCs occurring at different time scales during the degradation [30]. In this work, IS analysis was used to study the photostability of the inverted PTB7-Th:PC$_{70}$BM-based solar cells under the exposure of 1 sun illumination (standard reference AM 1.5G) and 1000 lux artificial LED 2700 K light over aging time. Standard procedures of ISOS L-1 and low-light measurement protocols were used for an accurate lifetime determination [31]. The cell reached a max PCE of 16.19% by illuminating the PSCs cells under LED light and showed close to 12 times prolonged lifetimes (3060 min) relative to the cells illuminated under full sunlight. The photodegradation behaviors of the devices studied by impedance spectroscopy reveal that the main cause behind the instability is the electron transport layer.

II. EXPERIMENTAL DETAILS

As illustrated in the inset Fig. 1a, the studied devices were fabricated using an inverted structure consisting of
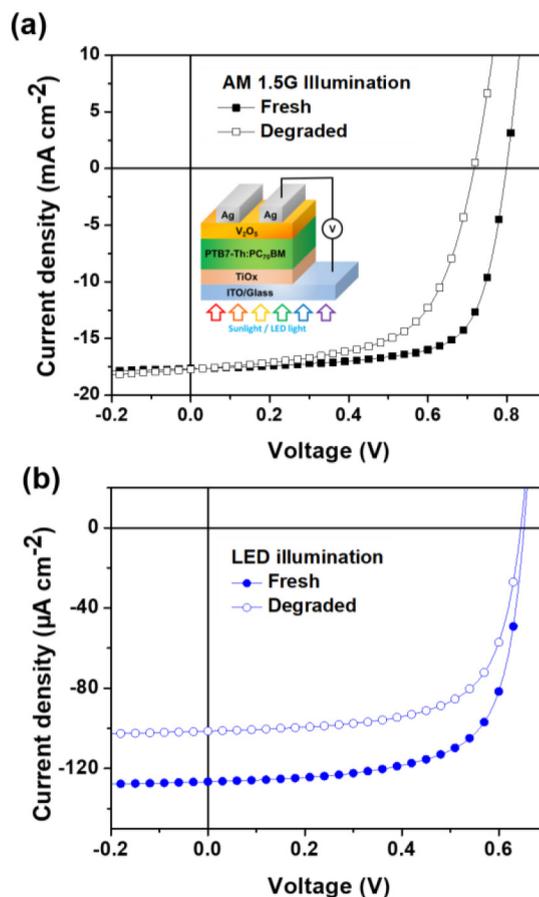
FIGURE 1. Illuminated current density-voltage (*J* − *V*) characteristics of fresh (solid symbol) and degraded (open symbol) cells exposed under (a) AM 1.5G and (b) 1000 lux LED 2700 K irradiation. The light intensity of AM 1.5G spectrum is 100 mW cm^{-2} and 1000 lux LED 2700 K spectrum is 0.35 mW cm^{-2}. The inset figure is the architecture of inverted PTB7-Th:PC$_{70}$BM-based devices fabricated in this study.

ITO/TiO$_x$/PTB7-Th:PC$_{70}$BM/V$_2$O$_5$/Ag. Inverted PSCs were chosen because they could enhance device performance and increase device stability than conventional PSCs [34]. The ITO-patterned glass substrates were first cleaned with a surface-active detergent and then sonicated in acetone, methanol, and isopropanol solvents for sequentially 10 min. Afterward, ITO substrates were dried in an oven at 100°C for 5 min, followed by ultraviolet-ozone treatment for 15 min. TiO$_x$, used as the electron transport layer (ETL), was synthesized by the sol-gel method following the previous work [14], [32], [33]. The TiO$_x$ precursor solution was diluted in anhydrous methanol with a volume ratio of 1:6 and spin-coated on the top of the ITO substrate at 6000 rpm. Subsequently, the TiO$_x$ films were thermally annealed at 400°C for 5 min to obtain 15 nm film thickness. The active layer solution, made by dissolving PTB7-Th:PC$_{70}$BM (1:1.5 w/w) in chlorobenzene:DIO (97:3% v/v) with a total concentration of 25 mg mL^{-1}, were stirred and heated at 40°C for 18 h and left aging for 48 h. The filtered aging solution was spin-coated onto the TiO$_x$ film at 750 rpm for

TABLE 1. Photovoltaic parameters of PTB7-Th:PC$_{70}$BM–based solar cells just after fabrication under different light sources illumination.

Light sources	V_{OC} [V]	J_{SC} [mA cm^{-2}]	FF [%]	PCE [%]
AM 1.5G T$_0$	0.79 ± 0.01	17.13 ± 0.40	71.40 ± 0.42	9.64 ± 0.20
AM 1.5G T$_{80}$	0.72 ± 0.01	17.88 ± 0.35	59.74 ± 3.03	7.70 ± 0.52
LED 1000 lux T$_0$	0.65 ± 0.01	0.13 ± 0.01	65.60 ± 2.94	15.70 ± 0.40
LED 1000 lux T$_{80}$	0.65 ± 0.01	0.10 ± 0.01	66.59 ± 0.47	12.53 ± 0.34

TABLE 2. Summary of photostability lifetime of the fabricated cells degraded under AM 1.5G and 1000 lux LED light illumination.

Standard lifetime	AM 1.5G	LED 1000 lux
E$_0$, T$_0$ (PCE,%)	9.98	16.19
T$_{95}$ (min)	30	40
T$_{90}$ (min)	60	260
T$_{85}$ (min)	180	1020
T$_{80}$ (min)	260	3060

30 sec, yielding an active layer thickness of 100 nm. V$_2$O$_5$ (5 nm) and Ag (100 nm) as the hole transport layer and top electrodes were sequentially deposited through a shadow mask under high vacuum conditions ($\leq 1 \times 10^{-6}$ mbar). The effective area for all devices was 0.09 cm^2. All fabrication process was carried out under nitrogen environment.

The degradation study was carried out at room temperature under an inert environment using two different light sources: solar simulator AM 1.5G (100 mW cm^{-2}) and an artificial LED 2700 K light (1000 lux = 0.35 mW cm^{-2}), following the International Summit on OSC Stability ISOS standard L-1 and low-light measurements [31]. The current density–voltage (*J-V*) characteristics of PSCs devices were performed using a solar simulator (Abet Technologies model 11 000 class type A, Xenon arc) and LED lamp (warm white lamp with a color temperature of 2700 K Philips A60 13W E27, Philips, Netherlands) using a Keithley 2400 source-measure unit under dark and illumination conditions. The light intensity of the AM 1.5G spectra was calibrated by an NREL certified monocrystalline silicon photodiode, while those of LED spectra were calibrated by a silicon-cell pyranometer (model MP-100, Apogee Instruments, Inc.) with a calibration factor of 5.0 W m^{-2} mV^{-1}. The illuminance of LED lamp was measured by a digital light meter (Spectra Cine, Candela II-A, Model C-2010 EL). The constant illumination was maintained by warmed the LED lamp up for 30 min and kept the distance between the devices and the light source. The spectra of AM 1.5G and LED light are displayed in Fig. S1 in supplementary material. Impedance spectroscopy measurement was performed under AM 1.5G and LED 2700 K illumination using HP-4192A impedance analyser in the frequency range between 1 Hz and 10 MHz.

III. RESULTS AND DISCUSSION

In this work, we study the device performance, photostability lifetime, and degradation behavior of the cells exposed under continuous illumination of two different light sources, standard reference AM 1.5G (100 mW cm^{-2}) and 1000 lux LED 2700 K lamp (0.35 mW cm^{-2}) in inert atmosphere. Fig. 1 shows the illuminated current density-voltage (*J − V*) characteristics of the studied devices before and after the photo-aging test. It can be observed that the *J − V* curve for the degraded cell under AM 1.5G illumination (Fig. 1a) was shifted to lower open-circuit voltage (V$_{OC}$), while the degraded cell under LED illumination (Fig. 1b) shows a more

pronounced shift to the lower short-circuit current density (J$_{SC}$) respect to the fresh cells. More detailed photovoltaic parameters values are summarized in Table 1, where all numbers represent the average and standard deviation values from four cells in each group. The dark *J − V* characteristics of these devices are displayed in the supporting information (Fig. S2 in supplementary material and Table SI in supplementary material).

In agreement with prior work [32], a max PCE of the fresh device under 1 sun illumination was 10% with the average PCE of 9.64%, a V$_{OC}$ of 0.79 V, a J$_{SC}$ of 17.13 mA cm^{-2}, and a fill factor (FF) of 71.4%. On the other hand, the fresh cells illuminated under LED light have a PCE about 1.6 times higher than that of 1 sun-illuminated cells, showing the highest PCE of 16.19% with an average PCE of 15.7%, a V$_{OC}$ of 0.65 V, a J$_{SC}$ of 0.13 mA cm^{-2}, and an FF of 65.6%. The PCE enhancement of the PSCs cells illuminated under LED light is in good agreement with the related studies using PTB7-Th:PC$_{70}$BM as the photoactive materials [10], [35], [36]. It may be due to the well-match between the absorption photoactive spectra of PSCs with the emission spectra of the LED spectrum. The LED light was employed because it provides low power consumption as a versatile light source, which is reckoned to be widely used for the industrial and domestic household [37].

To investigate the effect of different light source illumination on the photodegradation mechanism of the studied devices, the photo-aging test was conducted in an inert atmosphere (<0.1 ppm O$_2$ and <0.1 ppm H$_2$O) under continuous illumination of standard 1 sun and 1000 lux LED light. In an inert environment, the degradation due to ambient moisture and oxygen can be avoided, giving a less significant effect on the studied photostability mechanism. Fig. 2 shows the performance parameters of the devices: PCE, J$_{SC}$, V$_{OC}$, and FF over the aging time, normalized to their initial values. Following the ISOS-L-1 and low light measurement protocols, the device lifetimes are listed in Table 2. The photo-aging test was carried out until the PCE of the cells decays 20% from its initial value, known as E$_{80}$, T$_{80}$. The initial PCE (E$_0$) and the times T$_{95}$, T$_{90}$, and T$_{85}$ defined in the protocols [31] are also shown in the table. After reaching T$_{80}$, we found that the lifetimes of the cells aged under LED illumination are almost 12 times longer than under AM 1.5G solar simulator. It indicates a vivid effect of different light source illumination on the photodegradation pathways of PSCs.
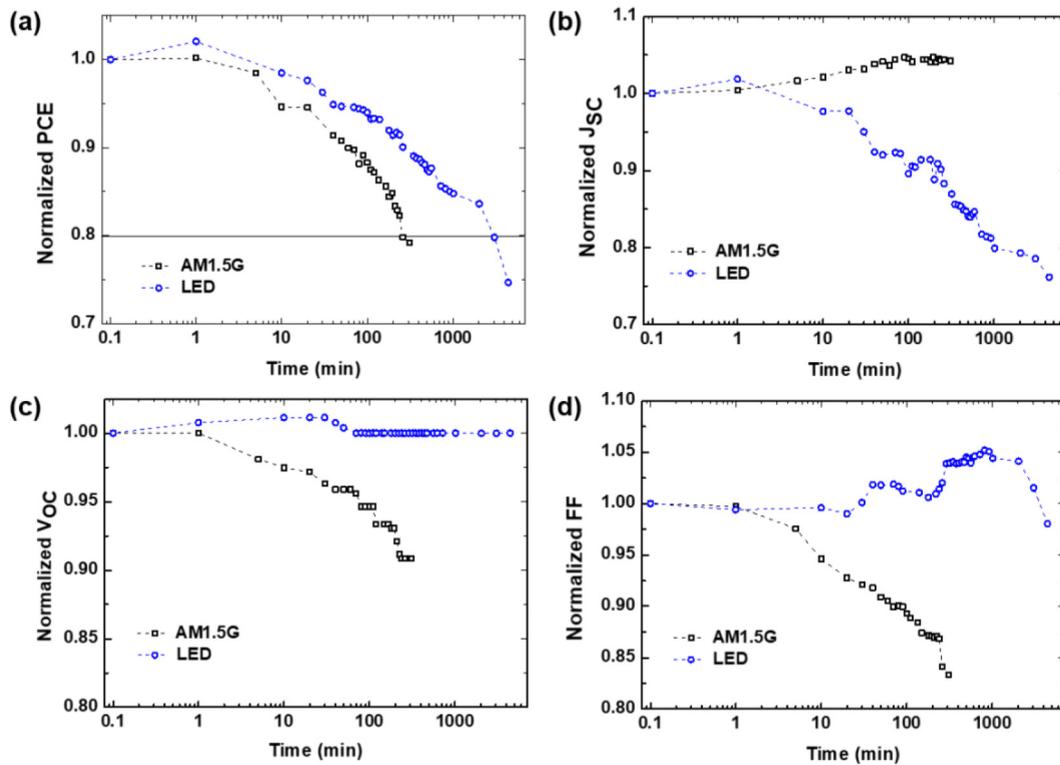
FIGURE 2. Normalized device performance parameters (a) PCE, (b) J_{SC}, (c) V_{OC}, and (d) FF of inverted PTB7-Th:PC$_{70}$BM-based device under two light sources exposure: AM 1.5G solar simulator (black squares) and 1000 lux LED lamp (blue circle).

As presented in Fig. 2a, the PCEs for all cells decrease exponentially over the degradation time. The PCE of LED-aged cells dropped 20% after 3,060 min of continuous illumination, while those of 1 sun-aged cell reaches its T$_{80}$ only in 260 min. Rapid decay of all of the studied PSCs devices in the first few minutes are observed in Fig. S3 in supplementary material. This phenomenon is often reported as a "burn-in loss" degradation mechanism due to the photochemical reaction within the device layers and the presence of processing additive 1,8-diiodooctane as photo-acid [38]–[40].

Fig. 2b presents the normalized J_{SC} values for two different light sources photo-aging over the degradation time. At T$_{80}$, the devices illuminated under AM 1.5G solar simulator show an increasing J_{SC} 4% higher in respect of its initial value. That increment may arrive from the UV-irradiation dependence, known as light-soaking effect, when the UV components from the solar simulator spectrum irradiate the cells. The light-soaking phenomenon in inverted PSCs employing TiOx or the other metal-oxides materials as ETL has been widely observed [41]. It may originate from the photoinduced rearrangement of the Fermi levels at indium tin oxide/TiOx interface, as reported elsewhere [42], [43]. On the contrary, the J_{SC} of LED-aged cells fell 21% at T$_{80}$. The J_{SC} decay under LED illumination originates from the absence of UV components in the LED spectrum. This behavior correlates well with the PCE behavior over the photo-aging time.

The normalized V_{OC} over the photo-aging time is presented in Fig. 2c. The sun-aged cells show decreased values of around 10% after they reached T$_{80}$. V_{OC} losses may arise from light-induced trap states/defects, as described elsewhere [23]. Different behavior was observed in LED-aged cells, and their V_{OC} start to increase slightly until 30 min and remain stable after 50 min. The other performance parameters that need to take into account is FF, as shown in Fig. 2d. Normalized FF of sun-aged devices decreases abruptly around 16% of its initial value until T$_{80}$. On the other hand, the FF values of LED-aged cell have followed the trend: stable for a long time, decrease for a short time, suddenly increased, and continue following the same trend until it has decreased up to its initial value at T$_{80}$.

To examine the charge carrier recombination mechanisms within the devices, the dependency of the J_{SC} and V_{OC} on light intensity (P_{light}) was measured and the results are shown in Fig. 3. The J_{SC} generally follows a power-law dependence upon P_{light}, as described by the expression:

$$J_{SC} \propto P_{light}^{S1} \qquad (1)$$

where *S1* represents a power-law exponent. For bulk heterojunction polymer/fullerene-based solar cells, *S1* ranges typically from 0.85 to 1 [44]. A linear dependence was observed when the value of *S1* close to 1 indicates weak bimolecular recombination. Conversely, a value of *S1* smaller than 1 suggests that bimolecular recombination of free charge carriers can limit the photocurrent devices [45]. Figs. 3a and
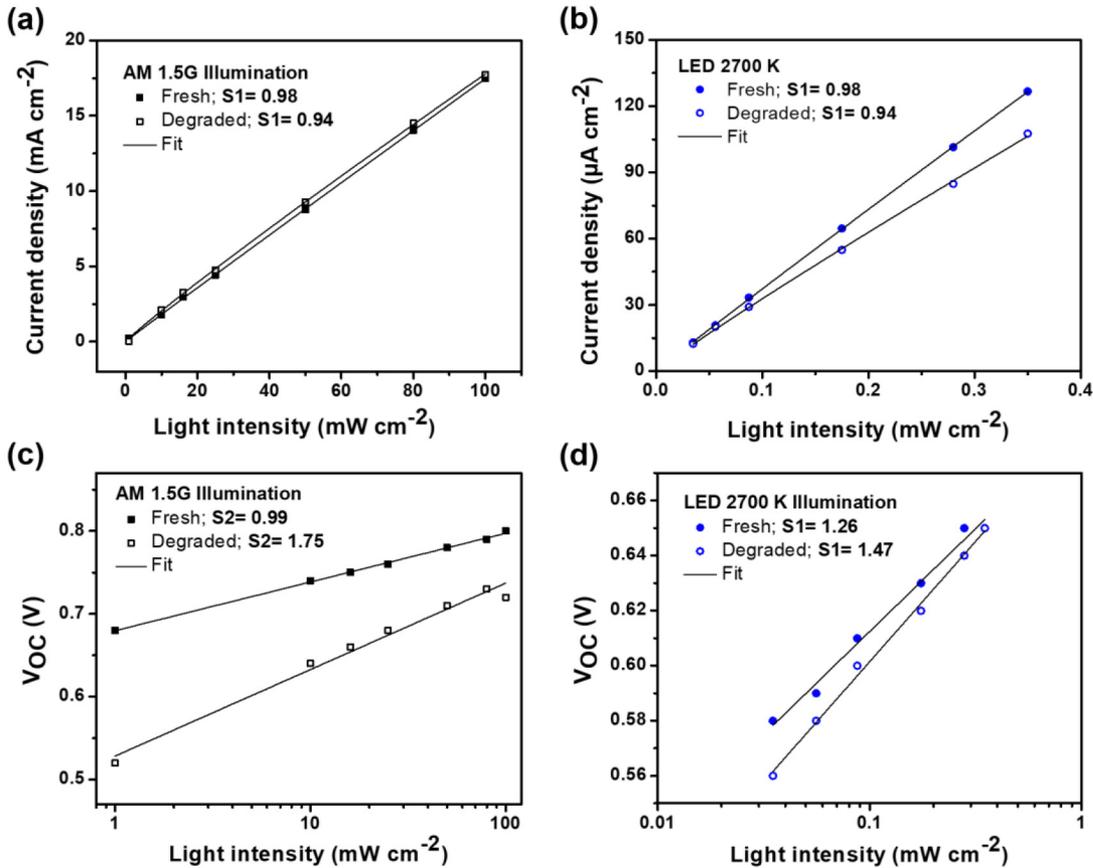
FIGURE 3. (a,b) J_{SC} and (c,d) V_{OC} dependence on light intensity over aging time of inverted PTB7-Th:PC$_{70}$BM-based device under (a,c) AM 1.5G and (b) 1000 lux LED light illumination. All measurements were carried out in an inert atmosphere.

b show the plots of J_{SC} vs P_{light} for the cells illuminated under solar irradiation ($10 - 100$ mW cm^{-2}) and 1000 lux LED light intensity (<1 mW cm^{-2}). It is apparent that the slope is unity and is not influenced by different light sources exposure. All plots were fitted using equation 1. The similar fitted *S1* values for the fresh (0.98) and aged (0.94) cells illuminated under AM 1.5G and LED irradiation suggest that there is neither bimolecular recombination nor a build-up of space charge in all devices for both fresh and aged cells.

To gain more insight into recombination kinetics between the fresh and photo-aged PSCs, the logarithmic dependence of V_{OC} vs. P_{light} can be expressed using the expression derived from the Shockley diode equation as following [46]:

$$V_{oc} \propto S2 \frac{k_B T}{q} \ln(P_{opt}) \propto n \frac{k_B T}{q} \ln(J_{sc}) \qquad (2)$$

where n is the recombination ideality factor of the diode ($n = S2/S1$), k_B is the Boltzmann constant, T is the Kelvin temperature, and q is the elementary charge. Fig. 3c and d show semilogarithmic plots of V_{OC} versus P_{light} for fresh and aged-PSCs under both illumination. The fitted *S2* values were obtained from equation 2. The obtained *S2* values of 0.99 and 1.26 lead to obtained n values of 1.01 and 1.28 for

the fresh cells under 1 sun and 1000 lux LED light illumination, respectively. Furthermore, the increasing *S2* values were expected when we carried out the photoaging test. The solar-aged cells have *S2* values of 1.75 and the LED-aged cells of 1.47, resulting in n values of 1.86 and 1.38, respectively. This trend is coherent with the ideality factor of the diode obtained from the dark $J - V$ fitting model (n value in Table SI in supplementary material). These results are in the range of expected values since the ideality factor for PSCs ranges between 1 and 2 ($1 \leq n \leq 2$) [47]. Following theoretical considerations, the condition of n equal to 1 indicates the bimolecular recombination mechanism governs the charge recombination in PSCs, whereas when n near to 2, it is dominated by trap-assisted recombination mechanism [40]. In addition, the increase from $n = 1$ to $n = 2$ indicates the increasing trap density, as observed in the solar-aged cells. A higher increased of n values of solar-aged cells ($n = 1.86$) from its fresh sample suggest the recombination losses in solar-aged cells are mainly due to band-trail trap states in bulk. It can explain a rapid decay of V_{OC} over the AM 1.5G aging time is due to the light-induced trap formation, as shown in Fig. 2c. On the other hand, the lower n values for LED-aged cells compare to their solar-aged counterpart can be attributed to low concentration traps
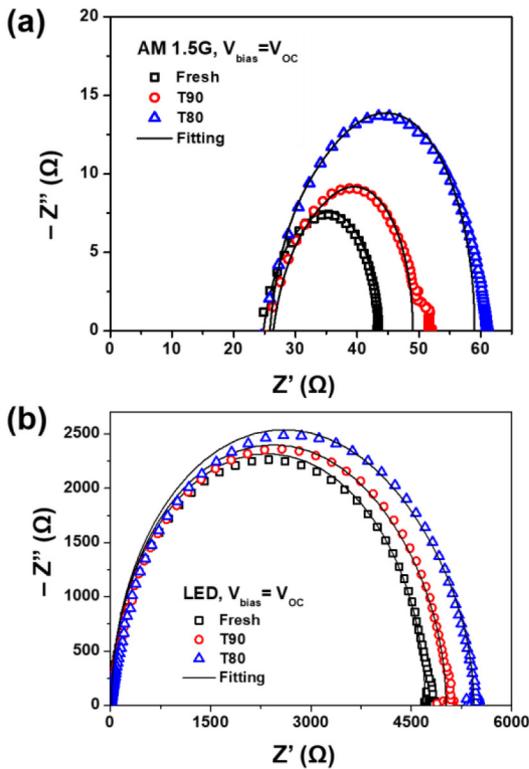
FIGURE 4. Cole-Cole plots at open-circuit voltage bias over aging time of PTB7-Th:PC$_{70}$BM-based devices under (a) AM 1.5G and (b) 1000 lux LED illumination. The experimental results were fitted using the 3RC circuit model (solid lines).

FIGURE 5. The percentage contribution of each layer resistance to the total resistance of the cells for fresh and degraded devices photodegraded under (a) standard AM 1.5G and (b) 1000 lux LED 2700K irradiation. The values were extracted by modeling the IS measurements at open-circuit conditions.

in bulk under low-light illumination, resulting in the most stable V$_{OC}$ values over the LED aging time (Fig. 2c).

In spite of the fact that $J - V$ curves could provide the information in which performance parameters were affected by photodegradation, they could not give concrete evidence to understand the detrimental cause of PSCs performance deterioration. It is because of the complexity of the photodegradation mechanism. Hence, impedance spectroscopy (IS) measurements were carried out under solar simulator and LED irradiation aging condition to gain more information on the photostability of PTB7-Th:PC$_{70}$BM-based devices. The IS measurements were performed under the frequency sweep from 1 Hz to 10 MHz over the aging time from T$_0$ up to T$_{80}$ at the open-circuit voltage bias, superimposing an AC signal with 50 mV amplitude. The experimental data were fitted by an equivalent electrical model using three resistor/capacitor (3RC) circuits in series, as shown in Fig. S4 in supplementary material. These elements are related to the series resistance of ITO and the resistance and capacitance of TiO$_x$, active layer, and V$_2$O$_5$. The geometrical capacitance values of each layer can be calculated theoretical capacitance and their values shown in Table SII in supplementary material.

Fig. 4 shows the Cole-Cole (Nyquist) plots of the impedance spectra of solar-aged and LED-aged PSCs measured at the open-circuit condition with their corresponding Bode plots in

Fig. S5 in supplementary material. It is observed that a single process represented by one arc behavior in the Cole-Cole plot and one maximum in the real and imaginary components of the Bode plots depend on the illumination condition given, high-frequency features under AM 1.5G illumination and low-frequency features under LED 1000 lux illumination. The important parameters that can be extracted from the Cole-Cole plots after fitting with the 3RC circuit model are the capacitance (C), resistance (R), and time constant (τ). It can be seen that all plots over the degradation time show typical arc behavior, indicates that the equivalent 3RC circuit model is suitable for these spectra. Moreover, the diameter of arc increases as the aging time increases, suggesting an increased bulk resistance of PTB7-Th:PC$_{70}$BM devices [29]. It is worth noting that the diameter of the arc is directly related to the value of the resistance. The extracted resistance values of the fitted data from solar-aged and LED-aged cells over the lifetime stability are listed in Tables SIII and SIV, respectively in supplementary material. It is observed that the LED-aged cells have orders of magnitude higher resistance than that of solar-aged cells. The higher resistances of LED-illuminated fresh and aged cells were mainly due to the bulk RC ladder under low-light conditions, as we report elsewhere [10].

Moreover, the fitting values of solar-illuminated fresh cells are dominated by ITO series resistance. Nevertheless, as the aging time increase, the measurement is strongly affected by TiO_x resistance.

To further analyze in which layer affects most the photodegradation under different light sources illumination, the percentage contribution of each layer resistance to the total resistance ($R_{tot} = R_S + R_{ETL} + R_{bulk} + R_{HTL}$) was investigated, as shown in Fig. 5. We found the $\Delta R_{layer}/R_{total}$ (R_{layer}/R_{total} of aged $- R_{layer}/R_{total}$ of fresh) of TiO_x is the highest among the other layers under both AM 1.5G and LED illumination. This result suggests that the performance deterioration of PSCs under both AM 1.5G and LED illumination is mainly due to the degradation of TiO_x layer. Such degradation may arise because of the photochemical activation when it is in operation [48].

IV. CONCLUSION

In conclusion, an electrical degradation study of the inverted structure of ITO/ETL/PTB7-Th:PC_{70}BM/V_2O_5/Ag PSCs photodegraded under two different light sources in an inert atmosphere was presented. A high PCE of up to 16.19% and a long operational lifetime T_{80} of 3060 min were achieved by LED-irradiated devices, higher and more stable than that of AM 1.5G-irradiated devices with PCE of 9.98% and T_{80} of only 260 min. Using impedance spectroscopy and three resistive-capacitive equivalent circuit models, we were able to reveal that the main source of the photodegradation in the PTB7-Th:PC_{70}BM-based device is the electron transport layer (TiO_x). Our results demonstrate that PSCs have potential practical applications as high performance and a high stable indoor power source.

REFERENCES

[1] R. Singh *et al.*, "Ternary blend strategy for achieving high-efficiency organic photovoltaic devices for indoor applications," *Chem. A Eur. J.*, vol. 25, no. 24, pp. 6154–6161, 2019.

[2] A. Al-Fuqaha, M. Guizani, M. Mohammadi, M. Aledhari, and M. Ayyash, "Internet of Things: A survey on enabling technologies, protocols, and applications," *IEEE Commun. Surveys Tuts.*, vol. 17, no. 4, pp. 2347–2376, 4th Quart., 2015.

[3] Y. Aoki, "Photovoltaic performance of organic photovoltaics for indoor energy harvester," *Org. Electron.*, vol. 48, pp. 194–197, Sep. 2017.

[4] K. Shafique, B. A. Khawaja, F. Sabir, S. Qazi, and M. Mustaqim, "Internet of Things (IoT) for next-generation smart systems: A review of current challenges, future trends and prospects for emerging 5G-IoT scenarios," *IEEE Access*, vol. 8, pp. 23022–23040, 2020.

[5] Y. Cui, L. Hong, and J. Hou, "Organic photovoltaic cells for indoor applications: Opportunities and challenges," *ACS Appl. Mater. Interfaces*, vol. 12, no. 35, pp. 38815–38828, 2020.

[6] Z. Ding, R. Zhao, Y. Yu, and J. Liu, "All-polymer indoor photovoltaics with high open-circuit voltage," *J. Mater. Chem. A*, vol. 7, no. 46, pp. 26533–26539, 2019.

[7] S. Kim, M. Jahandar, J. H. Jeong, and D. C. Lim, "Recent progress in solar cell technology for low-light indoor applications," *Current Altern. Energy*, vol. 3, no. 1, pp. 3–17, 2019.

[8] M. Freunek, M. Freunek, and L. M. Reindl, "Maximum efficiencies of indoor photovoltaic devices," *IEEE J. Photovolt.*, vol. 3, no. 1, pp. 59–64, Jan. 2013.

[9] R. Steim *et al.*, "Organic photovoltaics for low light applications," *Sol. Energy Mater. Sol. Cells*, vol. 95, no. 12, pp. 3256–3261, 2011.

[10] A. A. A. Torimtubun, J. G. Sánchez, J. Pallarès, and L. F. Marsal, "A cathode interface engineering approach for the comprehensive study of indoor performance enhancement in organic photovoltaics," *Sustain. Energy Fuels*, vol. 4, no. 7, pp. 3378–3387, 2020.

[11] M. Nam *et al.*, "Ternary organic blend approaches for high photovoltaic performance in versatile applications," *Adv. Energy Mater.*, vol. 9, no. 38, 2019, Art. no. 1901856.

[12] M. Jørgensen, K. Norrman, and F. C. Krebs, "Stability/degradation of polymer solar cells," *Sol. Energy Mater. Sol. Cells*, vol. 92, no. 7, pp. 686–714, 2008.

[13] S. A. Gevorgyan *et al.*, "Lifetime of organic photovoltaics: Status and predictions," *Adv. Energy Mater.*, vol. 6, no. 2, pp. 1–17, 2016.

[14] J. G. Sánchez *et al.*, "Stability study of high efficiency polymer solar cells using TiO_x as electron transport layer," *Sol. Energy*, vol. 150, pp. 147–155, Jul. 2017.

[15] L. Duan and A. Uddin, "Progress in stability of organic solar cells," *Adv. Sci.*, vol. 7, no. 11, 2020, Art. no. 1903259.

[16] W. R. Mateker and M. D. McGehee, "Progress in understanding degradation mechanisms and improving stability in organic photovoltaics," *Adv. Mater.*, vol. 29, no. 10, 2017, Art. no. 1603940.

[17] V. S. Balderrama *et al.*, "Degradation of electrical properties of PTB1: PCBM solar cells under different environments," *Sol. Energy Mater. Sol. Cells*, vol. 125, pp. 155–163, Jun. 2014.

[18] I. I. Jeon and Y. Matsuo, "Vertical phase separation and light-soaking effect improvements by photoactive layer spin coating initiation time control in air-processed inverted organic solar cells," *Sol. Energy Mater. Sol. Cells*, vol. 140, pp. 335–343, Sep. 2015.

[19] A. Uddin, M. B. Upama, H. Yi, and L. Duan, "Encapsulation of organic and perovskite solar cells: A review," *Coatings*, vol. 9, no. 2, pp. 1–17, 2019.

[20] L. N. Inasaridze *et al.*, "Light-induced generation of free radicals by fullerene derivatives: An important degradation pathway in organic photovoltaics?" *J. Mater. Chem. A*, vol. 5, no. 17, pp. 8044–8050, 2017.

[21] N. Y. Doumon, G. Wang, L. J. A. Koster, and R. C. Chiechi, "Relating polymer chemical structure to the stability of polymer: Fullerene solar cells," *J. Mater. Chem. C*, vol. 5, no. 26, pp. 6611–6619, 2017.

[22] G. Williams and H. Aziz, "Implications of the device structure on the photo-stability of organic solar cells," *Sol. Energy Mater. Sol. Cells*, vol. 128, pp. 320–329, Sep. 2014.

[23] N. Gasparini *et al.*, "Exploiting ternary blends for improved photostability in high-efficiency organic solar cells," *ACS Energy Lett.*, vol. 5, no. 5, pp. 1371–1379, 2020.

[24] L. Duan *et al.*, "Comparative analysis of burn-in photo-degradation in non-fullerene COi8DFIC acceptor based high-efficiency ternary organic solar cells," *Mater. Chem. Front.*, vol. 3, no. 6, pp. 1085–1096, 2019.

[25] C. H. Peters *et al.*, "The mechanism of burn-in loss in a high efficiency polymer solar cell," *Adv. Mater.*, vol. 24, no. 5, pp. 663–668, 2012.

[26] J. Kong *et al.*, "Long-term stable polymer solar cells with significantly reduced burn-in loss," *Nat. Commun.*, vol. 5, pp. 1–8, Dec. 2014.

[27] A. Pockett, H. K. H. Lee, B. L. Coles, W. C. Tsoi, and M. J. Carnie, "A combined transient photovoltage and impedance spectroscopy approach for a comprehensive study of interlayer degradation in non-fullerene acceptor organic solar cells," *Nanoscale*, vol. 11, no. 22, pp. 10872–10883, 2019.

[28] M. Neukom, S. Züfle, S. Jenatsch, and B. Ruhstaller, "Opto-electronic characterization of third-generation solar cells," *Sci. Technol. Adv. Mater.*, vol. 19, no. 1, pp. 291–316, 2018.

[29] E. Osorio *et al.*, "Degradation analysis of encapsulated and nonencapsulated TiO_2/PTB7: PC_{70}BM/V_2O_5 solar cells under ambient conditions via impedance spectroscopy," *ACS Omega*, vol. 2, no. 7, pp. 3091–3097, 2017.

[30] E. Von Hauff, "Impedance spectroscopy for emerging photovoltaics," *J. Phys. Chem. C*, vol. 123, no. 18, pp. 11329–11346, 2019.

[31] M. O. Reese *et al.*, "Consensus stability testing protocols for organic photovoltaic materials and devices," *Sol. Energy Mater. Sol. Cells*, vol. 95, no. 5, pp. 1253–1267, 2011.

[32] A. A. A. Torimtubun, J. G. Sánchez, J. Pallarès, and L. F. Marsal, "Study of the degradation of PTB7-Th: PC70BM-based solar cells using TiOx as electron transport layers under ambient environment," in *Proc. Lat. Am. Electron Devices Conf.*, 2020, pp. 22–25.

[33] J. G. Sánchez, A. A. A. Torimtubun, V. S. Balderrama, M. Estrada, J. Pallares, and L. F. Marsal, "Effects of annealing temperature on the performance of organic solar cells based on polymer: Non-fullerene using V2O5 as HTL," *IEEE J. Electron Devices Soc.*, vol. 8, pp. 421–428, Oct. 2020.

[34] Y. Wang, H. Cong, B. Yu, Z. Zhang, and X. Zhan, "Efficient inverted organic solar cells based on a fullerene derivative-modified transparent cathode," *Materials*, vol. 10, no. 9, p. 1064, 2017.

[35] S. Mori, T. Gotanda, Y. Nakano, M. Saito, K. Todori, and M. Hosoya, "Investigation of the organic solar cell characteristics for indoor LED light applications," *Jpn. J. Appl. Phys.*, vol. 54, no. 7, 2015, Art. no. 071602.

[36] C. L. Cutting, M. Bag, and D. Venkataraman, "Indoor light recycling: A new home for organic photovoltaics," *J. Mater. Chem. C*, vol. 4, no. 43, pp. 10367–10370, 2016.

[37] B. Gayral, "Les LEDs pour l'éclairage: Physique de base et perspectives pour les économies d'énergie," *Comptes Rendus Phys.*, vol. 18, nos. 7–8, pp. 453–461, 2017.

[38] A. Sacramento, M. Ramírez-Como, V. S. Balderrama, S. I. Garduño, M. Estrada, and L. F. Marsal, "Degradation study of inverted polymer solar cells using inkjet printed ZnO electron transport layer," in *Proc. Lat. Amer. Electron Devices Conf.*, 2019, pp. 1–4.

[39] N. Y. Doumon, G. Wang, X. Qiu, A. J. Minnaard, R. C. Chiechi, and L. J. A. Koster, "1,8-diiodooctane acts as a photo-acid in organic solar cells," *Sci. Rep.*, vol. 9, pp. 1–14, Mar. 2019.

[40] N. Gasparini *et al.*, "Burn-in free nonfullerene-based organic solar cells," *Adv. Energy Mater.*, vol. 7, no. 19, pp. 1–7, 2017.

[41] A. Sundqvist, O. J. Sandberg, M. Nyman, J.-H. Smått, and R. Österbacka, "Origin of the S-shaped JV curve and the light-soaking issue in inverted organic solar cells," *Adv. Energy Mater.*, vol. 6, no. 6, pp. 1–7, 2016.

[42] B. Ecker, H.-J. Egelhaaf, R. Steim, J. Parisi, and E. Von Hauff, "Understanding S-shaped current-voltage characteristics in organic solar cells containing a TiO$_x$ interlayer with impedance spectroscopy and equivalent circuit analysis," *J. Phys. Chem. C*, vol. 116, no. 31, pp. 16333–16337, 2012.

[43] J. Kim, G. Kim, Y. Choi, J. Lee, S. H. Park, and K. Lee, "Light-soaking issue in polymer solar cells: Photoinduced energy level alignment at the sol-gel processed metal oxide and indium tin oxide interface," *J. Appl. Phys.*, vol. 111, no. 11, Jun. 2012, Art. no. 114511.

[44] L. J. A. Koster, V. D. Mihailetchi, R. Ramaker, H. Xie, and P. W. M. Blom, "Light intensity dependence of open-circuit voltage and short-circuit current of polymer/fullerene solar cells," *Org. Optoelectron. Photon. II*, vol. 86, no.12, Art. no. 61922G, 2005.

[45] P. Hartnagel and T. Kirchartz, "Understanding the light-intensity dependence of the short-circuit current of organic solar cells," *Adv. Theory Simulat.*, vol. 3, no. 10, pp. 1–11, 2020.

[46] V. V. Brus, "Light dependent open-circuit voltage of organic bulk heterojunction solar cells in the presence of surface recombination," *Org. Electron.*, vol. 29, pp. 1–6, Feb. 2016.

[47] M. Chegaar, A. Hamzaoui, A. Namoda, P. Petit, M. Aillerie, and A. Herguth, "Effect of illumination intensity on solar cells parameters," *Energy Procedia*, vol. 36, no. 36, pp. 722–729, 2013.

[48] J. Razzell-hollis, J. Wade, W. C. Tsoi, Y. Soon, J. Durrant, and J.-S. Kim, "Photochemical stability of high efficiency PTB7: PC70BM solar cell blends," *J. Mater. Chem. A*, vol. 2, no. 47, pp. 20189–20195, 2014.